Original Manuscript

JOURNAL OF COMPOSITE MATERIALS

Journal of Composite Materials
2023, Vol. 0(0) 1–13


Article reuse guidelines:
sagepub.com/journals-permissions
DOI: 10.1177/00219983231194391
journals.sagepub.com/home/jcm
Sage

Effects of thermal process conditions on crystallinity and mechanical properties in material extrusion additive manufacturing of discontinuous carbon fibre reinforced polyphenylene sulphide composites

Yahui Lyu[1], Jiang Wu[1], Haoqi Zhang[2], Conchúr M. Ó Brádaigh[1] and Dongmin Yang[1]

Abstract

This study investigates the thermal behaviour of discontinuous carbon fibre reinforced polyphenylene sulphide (CF/PPS), additively manufactured by material extrusion, with a focus on the effects of thermal process conditions on the degree of crystallinity, oxidation crosslinking and mechanical properties of CF/PPS from filament fabrication, material extrusion to annealing treatment. The screw extrusion parameters are optimised by performing a thermal analysis of the fabricated filaments. The effect of crosslinking reactions on the crystallinity process in determining the mechanical properties of the printed samples is illustrated by investigating the influence of the printing conditions. Furthermore, the effect of annealing treatment on the semi-crystalline polyphenylene sulphide (PPS) is studied by measuring the degree of crystallinity and viscoelasticity behaviours. Results demonstrate that the flexural properties of the printed CF/PPS composites at elevated processing temperatures are determined by the oxidation crosslinking between PPS chains. These enhance the crystallisation process of semi-crystalline polymers by acting as the nucleating agent first but negatively affect the mechanical properties at higher temperatures because of the detrimental effects of the polymer inter-chain bonding. The maximum flexural strength of printed CF/PPS reached 164.65 MPa when processing at an extrusion temperature of 280°C, a printing temperature of 320°C, and an annealing temperature of 130°C for 6 h. By adjusting the thermal treatment conditions, the degree of the crystallinity and the mechanical properties of the printed CF/PPS composites can be designed, controlled and tailored.

Keywords

Material extrusion additive manufacturing, carbon fibre, polyphenylene sulphide, thermal process condition, crystallinity

Introduction

Thermoplastic composites have increasing applications due to their advantages of rapid cycle time, improved impact strength, recyclability, and unlimited shelf life as compared to thermoset composites.[1] For instance, the G650 business jet from Gulfstream adopts the lightweight carbon fibre/polyphenylene sulphide (CF/PPS) to form the tail section, which reduces 10% of the structural weight and 20% of the cost.[2] Polyphenylene sulphide (PPS) is a semi-crystalline matrix with a relatively high service temperature, exceptional mechanical strength, great chemical resistance, and good flame retardation,[3] and it is less expensive than other high-performance semi-crystalline polymers like polyether ether ketone (PEEK).[4] Thermoplastic composites manufactured by additive manufacturing (AM) such as material extrusion technique recently emerged due to their high flexibility in geometry, cost-effectiveness, and being free of multiple processing tools.[5,6] The most common polymers used in material extrusion based printing are acrylonitrile

[1]School of Engineering, Institute for Materials and Processes, University of Edinburgh, Edinburgh, UK
[2]Department of Mechanical Engineering, National University of Singapore, Singapore

Corresponding author:
Dongmin Yang, School of Engineering, Institute for Materials and Processes, University of Edinburgh, King's Building, Edinburgh EH9 3FB, UK.
Email: dongmin.yang@ed.ac.uk

Data Availability Statement included at the end of the article

butadiene styrene (ABS),[7] polylactic acid (PLA),[8] polyamide (PA),[9] and polyethylene terephthalate (PETG).[10] Short carbon fibre reinforced polymers offer the most accessible pathway toward large-scale, affordable and functional AM composites.[11] Mixing short carbon fibres in the PPS feedstock can increase the thermal conductivity and mechanical strength and stiffness while reducing the thermal expansion and residual stress in the printed composites.[12] Furthermore, short carbon fibres can improve friction and wear resistance, even compared with their continuous carbon fibre counterparts.[13] In general, higher fibre content and better-aligned short fibres in additive manufacturing lead to improved mechanical properties of printed composites.[14] Therefore, material extrusion of discontinuous CF/PPS composites with a high fibre volume is likely to grow in the automotive, electronics, and aerospace industries as well as other fields, due to its relatively low cost, accessible printing process, and feasible recycling process.

As a typical heat crosslinking, semi-crystalline polymer, the degree of crystallinity of PPS in the extruding and printing processes is affected by the complex thermal conditions including melting and deposition, which subsequently influence the tensile strength, fracture toughness, impact properties and other mechanical properties.[15] Previous studies on material extrusion of PPS focused on the printing parameters,[16] heat transfer,[17] layer adhesion,[18,19] rheological and thermal properties[20,21] of CF/PPS composites.[22] They found that the 3D printed composites could present a comparable property to extrusion-compression moulding due to highly aligned fibres but a poorer mechanical property to the injection moulding. Material extrusion additive manufacturing still faces challenges, however, to produce high-performance short CF/PPS composite parts for high-end applications because of the formation of the densely packed and ordered crystalline regions as well as thermal and oxidative responses.[23] Although there is limited literature on the thermal history in material extrusion of CF/PPS, several studies have been reported on pure PPS[24,25] and other semi-crystalline polymers such as PEEK[26] and PET.[27] Results show that printed parts with different degrees of crystallinity or different crystallinity regions in the same part can be designed and realized by controlling the heat treatment process. The above literature demonstrated that it is essential to analyse the thermal conditions on the performance of 3D printed semi-crystalline composites.

Previous studies have focused on various aspects of CF/PPS composites in material extrusion, including printing parameters, rheological and thermal properties, and mechanical performance. However, there is a need for further research to specifically investigate the thermal conditions and their effects on the degree of crystallinity and mechanical properties of CF/PPS composites. The present study, therefore, addresses this gap by investigating the thermal conditions, optimizing the mechanical properties, and exploring potential applications of CF/PPS composites in material extrusion. Firstly, this study aims to understand how the thermal history influences the resulting composites performance by examining the impact of different thermal processing conditions on the degree of crystallinity and mechanical properties of CF/PPS composites. Secondly, by systematically varying these conditions, we aim to optimize the mechanical properties of CF/PPS composites. By controlling the thermal parameters, such as filament fabrication temperature and annealing treatment parameters, we seek to tailor the degree of crystallinity and enhance the mechanical performance of printed parts. Lastly, this study is to identify potential applications for CF/PPS composites in high-end industries, such as aerospace, automotive, and electronics. By demonstrating the enhanced mechanical properties achieved through thermal optimization, we aim to display the suitability of CF/PPS composites for lightweight and high-performance components in these industries. Overall, the study contributes to the knowledge and understanding of the thermal behaviour and performance of CF/PPS composites in material extrusion additive manufacturing, which can have implications or optimizing processing parameters and improving the mechanical properties of printed parts. The aerospace, automotive, electronics and general manufacturing properties can benefit from the optimized CF/PPS composites produced through material extrusion, while the recyclability aspect aligns with sustainable manufacturing practices.

Materials and methods

Materials

In this study, the commercial product polyphenylene sulphide (PPS) pellets filled with 30% short carbon fibres (Torayca A630T-30V, Toray Industries Inc., Tokyo, Japan) were used to fabricate the 3D printing filament. The PPS powder used in the Fourier transform infrared spectroscopy (FTIR) characterisation was ground from the PPS pellets (Torelina A900, Toray Industries Inc., Tokyo, Japan).

Filament fabrication

The CF/PPS pellets were dried before extrusion in a furnace at 100°C for at least 3 h, using a lab-scale single screw extruder (Noztek Pro HT). In the extrusion process, the pellets were fed into the hopper and then processed through the heated nozzle, as shown in Figure 1(a). An extrusion speed of 2.5 m/min was applied, and a winding spool was placed at the end of the extruder to receive the filament. The diameter of the extruded filament was 1.6±0.1 mm.

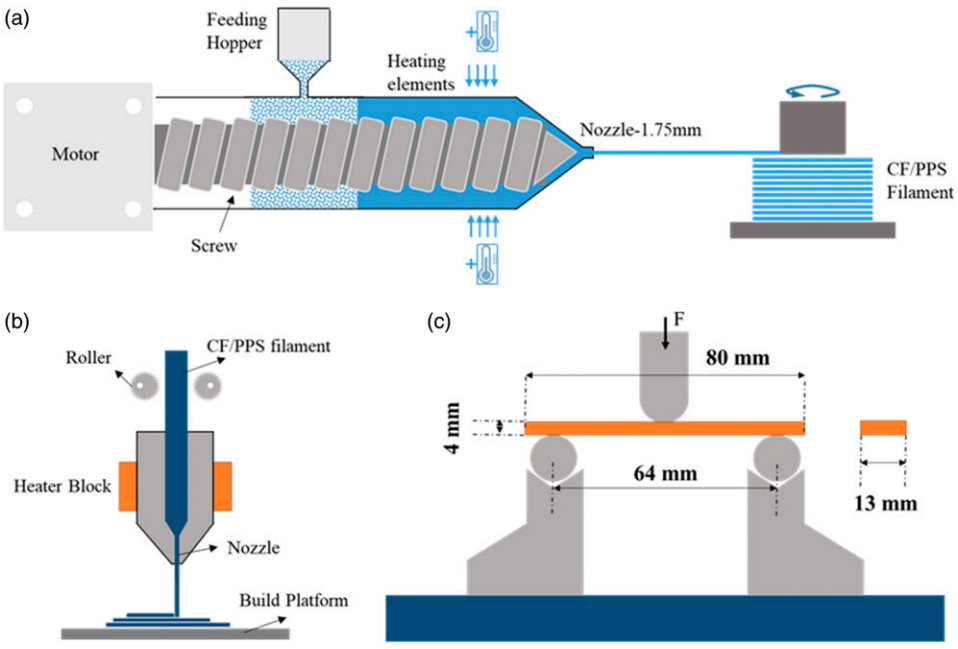

Figure 1. (a) Extrusion process of CF/PPS pellets; (b) Deposition process of the CF/PPS filament; (c) Three-point bending test set-up.

Material extrusion

A Creatbot F430 printer (420°C version, Henan, China) was used to print the CF/PPS filament, as shown in Figure 1(b). To optimise the printing conditions for the CF/PPS filaments, a range of nozzle temperatures between 310°C and 340°C were selected. It is noted that only the printing temperature was altered in this study. The build platform temperature was set to 90°C. The nozzle diameter is 0.8 mm, and the printing speed was 20 mm/s. The printing direction was set along the longitudinal direction. All specimens were printed to a 100% infill degree. In addition, the G-code was created by the slicer software Creatware, developed by Creatbot.

Three-point bending test

All the three-point bending tests on the printed parts were based on the ASTM D7264 standard. The tests were performed using an Instron 3369 machine with a 10 KN load cell. Each test was conducted under displacement control at a crosshead rate of 1.0 mm/min. According to the standard, rectangular parts with dimensions 80 mm × 13 mm × 4 mm were printed. This study tested three coupons within one group to mitigate the randomness. Figure 1(c) shows the three-point bending test setup.

Thermal characterisation

Thermal analysis of the CF/PPS composites was performed by differential scanning calorimetry (DSC, PerkinElmer 8000). All non-isothermal tests were carried out under a 20 mL/min nitrogen flow. The samples were heated up from 30°C to 300°C at a ramp rate of 20°C/min and then cooled down to 30°C at the same rate. After that, the samples were heated again based on the same program. Heat flows were measured in the first and second heating cycles for all the samples placed in the alumina crucibles. The melting temperature (T_m) was obtained from the second heating curve according to the heat capacity components, such as the reversing heat flow, while the total enthalpy of reaction in the melting process of the DSC curve was calculated automatically using the Pyris software to determine the crystallinity of the printed composites. The degree of crystallinity (X_c) of PPS is calculated by:

$$X_c(\%) = \frac{\Delta H_m}{\Delta H_f (1 - x)} \times 100\% \quad (1)$$

Where ΔH_m is the melting enthalpy, ΔH_f is the melting enthalpy of PPS with 100% crystallinity (80 J/g), both of which were obtained from the first heating run of the heat flow.[28] Note that the cold crystallisation process would not exist in the heating process based on the curves presented in the results section. Therefore, it was not necessary to consider this peak in the calculation.

Dynamic mechanical analysis

Dynamic mechanical analysis (DMA) is a technique to characterise the viscoelastic properties of a material by

subjecting the sample to a sinusoidal oscillating stress.[29] The viscoelastic properties of untreated printed CF/PPS parts and annealed printed CF/PPS parts were measured on a TA Instruments Discovery DMA 850, with specimen dimensions of 65 mm × 12 mm × 4 mm. Samples in each group were printed in a row to mitigate the errors in the printing process. Two groups were studied to check the repeatability. Each DMA test was performed with a temperature sweep from 40°C to 250°C in the double cantilever mode, using a frequency of 1 Hz and an amplitude of 30 μm. A ramp rate of 2°C/min was used in a nitrogen environment to avoid any degradation.

Morphology analysis

Morphology of the raw pellets, extruded CF/PPS filament and printed composites were observed using a scanning electron microscope (SEM, HITACHI TM4000Plus) and an optical microscope (Zeiss Axioskop 2). The SEM images were observed to compare the volume fraction of carbon fibres, while the optical microscopic images were used to calculate the void content.[30] Specimens were extracted from raw pellets, from CF/PPS filaments extruded at different temperatures, and from 3D printed composites, which were subsequently sanded and polished. Images obtained from SEM and optical microscopy were analysed using ImageJ software. The area of carbon fibres and air voids was measured and averaged. To process the images in the software, a threshold was applied according to the pixel difference between carbon fibres and PPS as well as the air voids.

Fourier transform infrared spectroscopy

Fourier Transform Infrared (FTIR) spectroscopy was used to characterise the presence of the functional groups in the original pellets, the extruded filament, and the annealed parts for PPS materials. A Perkin-Elmer Frontier spectrometer with a universal ATR accessory was used for the FTIR scan. CF/PPS composites were replaced by pure PPS part with natural colour for this work, as it was difficult to obtain accurate FTIR results using this machine due to the inclusion of black carbon fibres. To ensure a good contact between the samples with the probe, thin PPS parts were used in the scan and each sample was scanned 32 times for wavenumbers between 4000 cm^{-1} and 500 cm^{-1}.

Results and discussion

Filament fabrication of CF/PPS pellets

Firstly, the thermal properties of the as-received PPS and CF/PPS materials were characterised by the DSC machine. The results are shown in Figure 2. The melting temperature of the PPS polymer matrix was 273°C, while the melting temperature of the CF/PPS composites was 283°C. Based on the previous studies related to the extrusion of semi-crystalline polymers, increased chain entanglements and a lower degree of crystallinity in the extruded filament would be more desirable to enable a better printability during the 3D printing.[27] In those cases, the viscosity of the material would become lower and thus more easily extruded through the nozzle of the printer. To optimise the extrusion temperature for the CF/PPS filament, DSC testing was carried out to determine the degree of crystallinity of the filament extruded at different temperatures, ranging from 280°C to 330°C. To promote the chain entanglements of PPS, the molar mass reduction during the extrusion needed to be mitigated by reducing the water adsorption. Therefore, all the pellets were dried at 100°C for at least 3 h in a furnace prior to the extrusion. The degree of crystallinity versus extrusion temperatures and the first heating running in DSC is plotted in Figure 3.

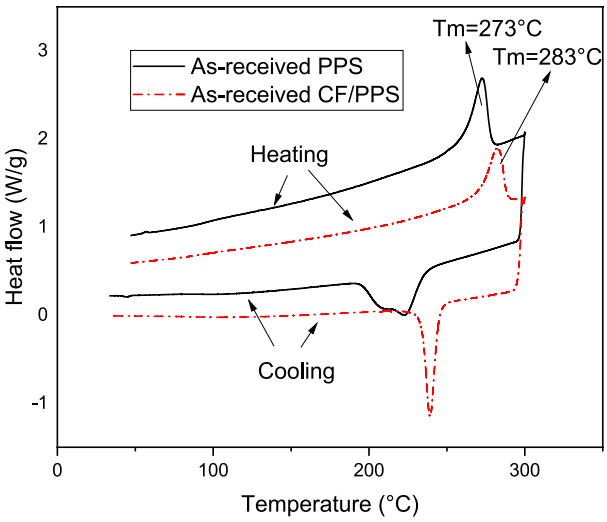

Figure 2. DSC curves of as-received PPS and CF/PPS.

The results illustrate that as the extrusion temperature increased from 280°C to 320°C, the degree of crystallinity increased from 28.3% to 51.4% accordingly and then showed a slight drop at 330°C. A more brittle filament with a higher crystallinity was obtained at a higher extrusion temperature. This is explained by more polymer chains folding and aligning themselves with each other as the temperature increases. The inter-chain bonding showed a slight decrease, however, when the filament was extruded at an elevated temperature, possibly because of oxidation. Therefore, the lowest extrusion temperature of 280°C was preferably selected to produce a more ductile and flexible filament for later 3D printing. A further decrease of the temperature below 280°C was impossible

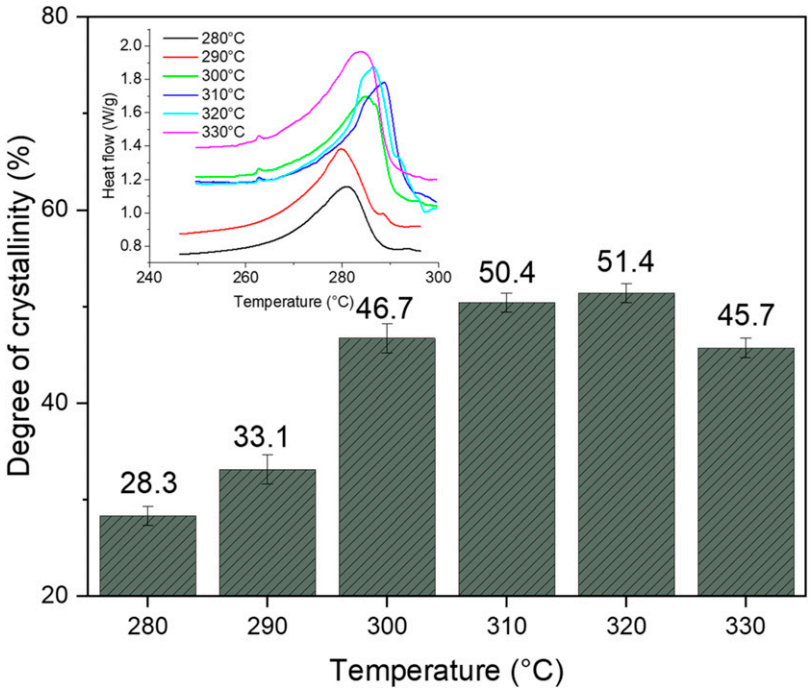

Figure 3. Degree of crystallinity of filaments extruded at different temperatures.

since the CF/PPS pellets could not be extruded at a temperature that is below the melting point of the PPS polymer. Overall, the optimal thermal conditions for the extrusion of CF/PPS pellets were identified as drying the pellets at 100°C for at least 3 h and then extruding at 280°C.

Material extrusion of CF/PPS filament

The printing parameters in material extrusion have a significant effect on the crystallisation behaviour of semi-crystalline polymers.[26] To investigate the optimal printing temperatures for the CF/PPS filament, the mechanical properties, as well as the crystallinity of the parts printed at 310°C, 320°C, 330°C and 340°C were studied. The crystallinity and DSC peaks of printed CF/PPS parts in the first heating process and the crystallinity temperatures at different printing temperatures are plotted in Figure 4. The relationship between the printing temperature and the mechanical properties in terms of flexural strength and modulus is presented in Figure 5.

As shown in Figure 4(a), when the temperature was increased from 310°C to 340°C, the crystallinity first increased from 48.7% to 51.5% at 320°C and then started to reduce until 340°C. At the same time, in the first cooling process shown in Figure 4(b), the crystallisation temperature of the CF/PPS reached a peak at 238.8°C first and then interestingly went down to 237.1°C. Correspondingly, the mechanical properties show the same trend, increasing from 125.3 MPa to 155.1 MPa for the flexural strength and from 10.64 MPa to 14.23 MPa for the flexural modulus and then decreasing to minimum values at 340°C (Figure 5). On one hand, the higher nozzle temperature provides more energy to melt all crystals in PPS material and allows more time for it to recrystallise in the cooling process during the 3D printing. In addition, PPS material tends to crosslink when the temperature is higher. This crosslinking may change the crystallisation process of uncross-linked PPS as a nucleating agent, which could provide the reaction point for the crystallisation process. The parts with higher crystallinity also manifest higher flexural strength and greater flexural modulus. On the other hand, when the nozzle temperatures are above 320°C, the effect of the nozzle temperature is more complicated.

PPS is known to be sensitive to oxidative reactions at process temperatures, which changes the behaviour of the polymer chains.[25] To better understand the chemical reactions between the PPS chains at higher temperatures, PPS parts printed at different nozzle temperatures were subjected to FTIR analysis. As seen in Figure 6, a new peak at 1042 cm^{-1} corresponding to the presence of aryl ether (C-O) bonding occurred at printing temperatures of 320°C, resulting from the oxidation reactions. And its intensity rose as the printing temperature increased. It is interesting to note that the cross-linking structure in the polymer acts as the nucleating agent first and then hinders the formation of the crystalline structure if the linkages become dominant at elevated temperatures.[31,32] These crosslinking chains could cause the deterioration

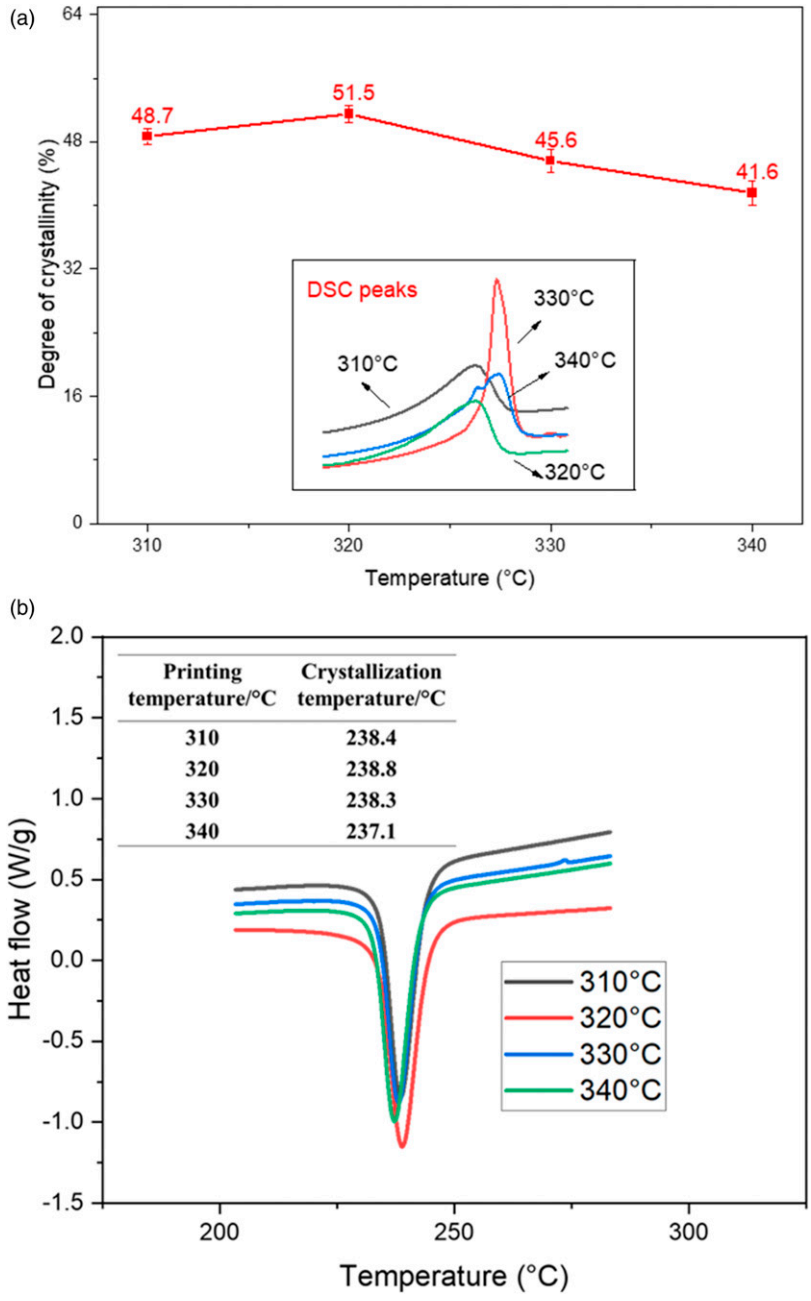

Figure 4. (a) Degree of crystallinity and DSC peaks of printed CF/PPS parts at different printing temperatures in the first heating process (b) crystallisation temperatures and DSC peaks of printed CF/PPS parts at different printing temperatures in the first cooling process.

phenomenon of polymer materials and then have a negative impact on crystallinity, thus reducing the mechanical properties of the printed parts. Results proved that the crosslinking effects performed a key role in determining the crystallinity in a higher nozzle temperature environment, and the degree of crystallinity indicated the mechanical properties. Overall, the optimal thermal process condition for this CF/PPS filament in material extrusion was found to be 320°C.

Heat treatment of 3D printed CF/PPS composites

It has been reported that heat treatment methods could have a significant effect on the degree of crystallinity of PPS polymers.[20] Therefore, furnace annealing could be an efficient method to enhance the crystallinity of the 3D-printed CF/PPS composites. The samples were annealed in a muffle furnace at 100°C for 45 min first and then at 130°C for 6 h. After annealing the samples were cooled down in the

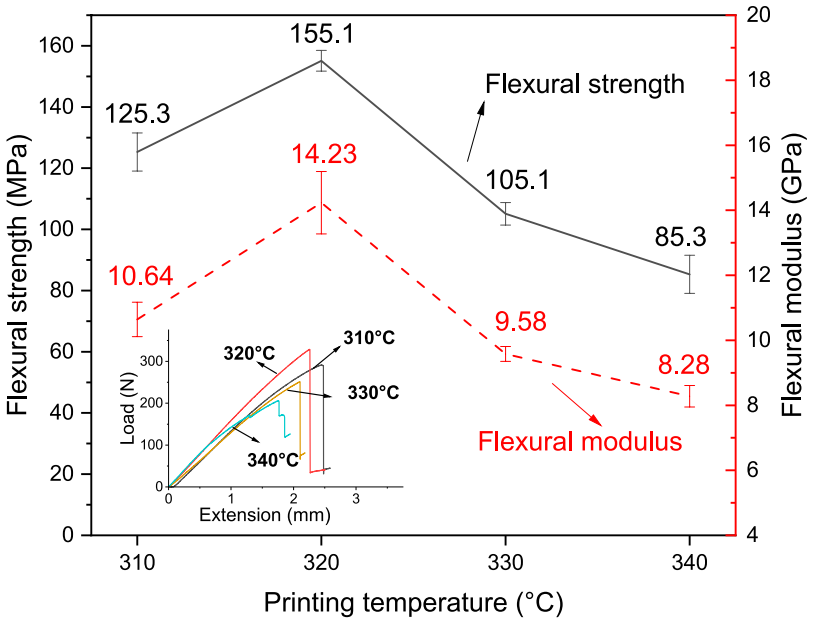

Figure 5. Flexural strength and modulus of printed CF/PPS parts at different printing temperatures.

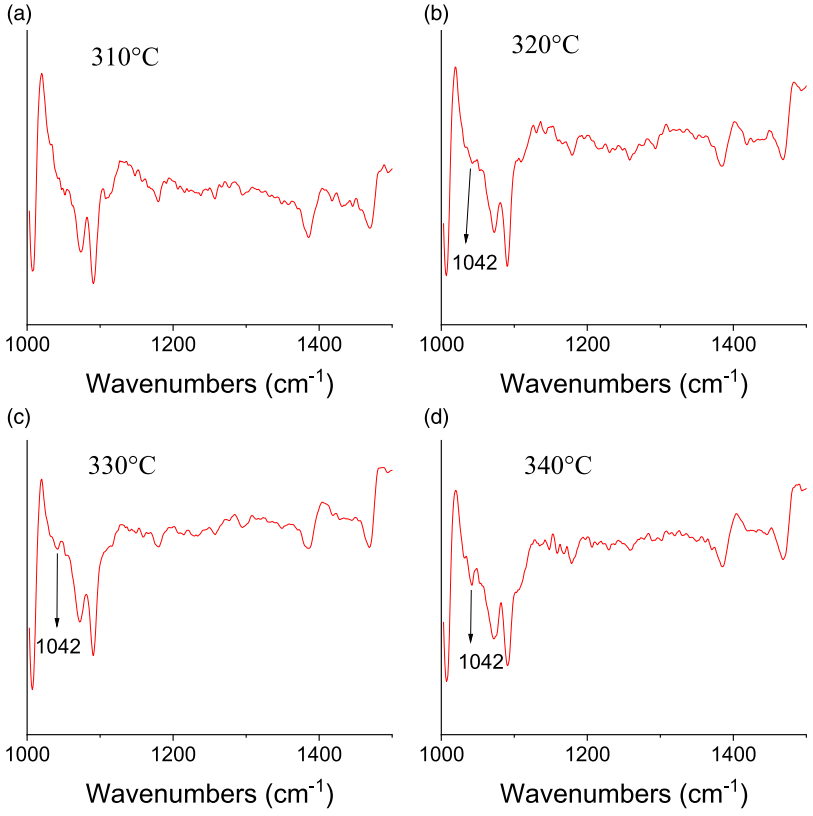

Figure 6. FTIR analysis of PPS parts at different printing temperatures: (a) 310°C; (b) 320°C; (c) 330°C and (d) 340°C.

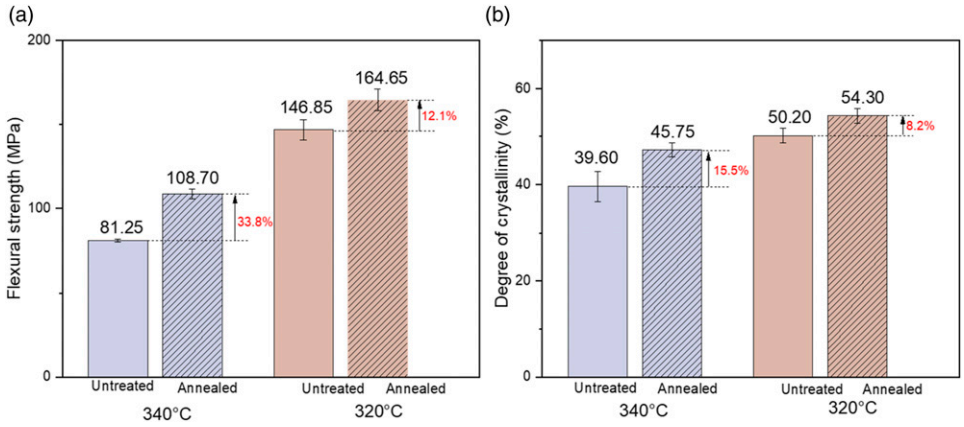

Figure 7. (a) Flexural strength and (b) degree of crystallinity of printed CF/PPS before and after annealing.

furnace naturally by air. Samples were 3D-printed at 320°C, the optimal printing temperature, and 340°C for comparisons. Half of the samples in each group were heat treated by annealing, and all samples were printed at one time to mitigate the uncertainties in the 3D printing process. The results were plotted in Figure 7.

As seen in Figure 7(a), the samples in both groups show an increase in flexural strength after the annealing treatment. When printing at 340°C, the annealed part showed an increase in flexural strength of 33.8%, in contrast to an increase of 12.1% for printing at 320°C. This is also confirmed by the curves in Figure 7(b) which show a higher degree of crystallinity after the annealing treatment. Annealed part printing at 320°C manifested the highest crystallinity of 54.3% after the treatment. It is known that the annealing method has a substantial impact on the crystallisation process, crystal structure, and size of the semi-crystalline polymers, resulting from the increase of chain mobility when heat is applied at temperatures above glass transition temperature and below melting temperature. In addition, isothermal annealing could also lead to structural changes in the form of chain extension, branching, or crosslinking (curing), especially in an oxidizing environment.[20,33,34] Therefore, the post-process heating treatment could increase the degree of crystallinity, trade off the printing defects and consequently improve the flexural properties of printed parts in this work. Annealing was found useful in improving the mechanical properties, especially for the parts with poorer mechanical performance. These findings provide insights in tailoring the mechanical properties of CF/PPS composites to meet specific application requirements.

DMA tests of two groups of the printed parts were conducted to measure the variation in viscoelastic properties with temperature for untreated and annealed samples of the printed CF/PPS composites to further understand the effect of the annealing treatment on the CF/PPS materials. The nozzle temperatures for these two samples are set to 320°C. Figure 8 depicts the storage modulus (G') as well as the damping factor (tan δ), which is the ratio of the loss modulus (G'') to the storage modulus (G'). The CF/PPS sample subjected to the annealing treatment shows an increased storage modulus from room temperature until 150°C. The G' was increased by 34.1%, the maximum value at *Tg* temperature (112°C) for annealed sample (Figure 8(a)). The storage modulus is indicative of the elastic energy stored in the material, which is related to the morphology changes of the material. In addition, the damping factor (tan δ) showed a reduction caused by annealing treatment in the same temperature range, which indicates that higher energy is used to deform the annealed materials that are directly dissipated into heat. These variations in storage modulus and damping factor are most likely to be generated by increasing crystallisation.[28] Greater constraints of polymer chains are imposed by more crystal domains and thereby reduce their mobility and increase the resistance to deformation caused by oscillating stress. As a result, the elasticity of the materials was improved.[33] Furthermore, Figure 8(b) shows that the *Tg* of the annealed samples has slightly increased by 8°C, resulting from this heating treatment method, which also is an indication of improved crystallinity in semi-crystalline PPS.

To confirm the presence of the oxidative groups in printing materials after annealing, untreated PPS and annealed PPS were characterised using FTIR, as shown in Figure 9. The peaks at 1572, 1470, and 1385 cm^{-1} were assigned to benzene ring stretching (C-C) in S–C_6H_4–S. The peaks at 1090 and 1072 cm^{-1} were attributed to ring-S stretching (C-S) in S–C_6H_4–S. The characteristic bands at 1008 cm^{-1} were attributed to C–H bending modes.[35,36] Compared with PPS raw material, there is a new peak at 1042 cm^{-1} generated by the aryl ether (C-O) linkage in the annealed sample, which indicates the oxidation reactions in the annealing process. In addition, the peak at 1178 cm^{-1} was broadened by the annealing treatment, corresponding to the stretching vibration adsorption of the –S=O.

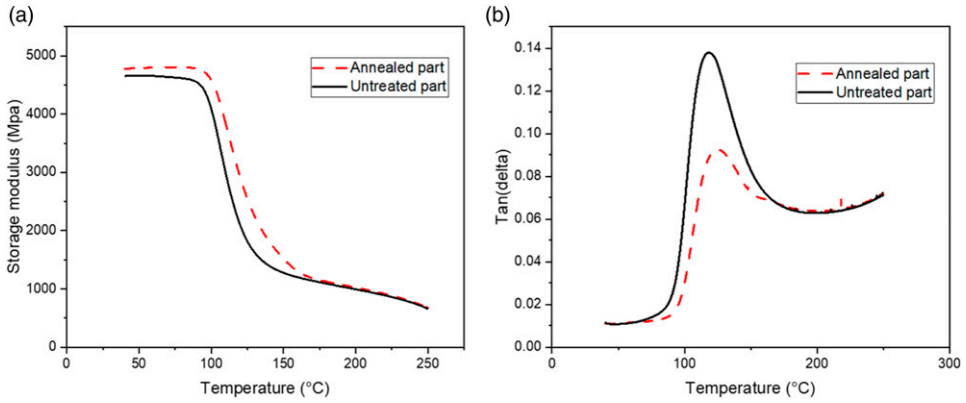

Figure 8. Comparison of storage modulus (a) and tan δ (b) for untreated printed parts and annealed parts.

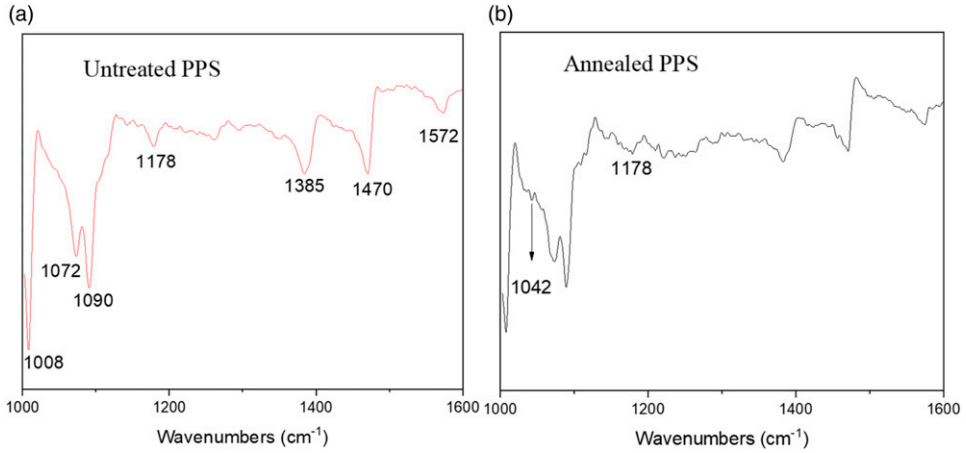

Figure 9. FTIR analysis of (a) untreated and (b) annealed PPS powders.

That indicates that the oxidation level was increased in the form of oxidative branching as well. In summary, the annealing treatment introduces the oxidative groups and increases the degree of crystallinity to the PPS material.

To compare the 3D printed CF/PPS in this study with previous work and PPS composites reinforced by random-oriented discontinuous carbon fibres in the literature, Figure 10 summarises published studies on the flexural strength and modulus of CF/PPS composites from both traditional manufacturing methods and material-extrusion additive manufacturing methods at different carbon fibre fractions.[3,13,37–42] Although there are limited studies on the material extrusion based additive manufacturing of short CF/PPS composites, there is a huge improvement (150%) in the flexural strength of PPS composites with 30.0 wt % fibres in this work compared with the previous 3D printed pure PPS parts, thanks to the carbon fillers. Meanwhile, the results in this work are comparable with the CF/PPS composites manufactured by the hydraulic press and injection moulding with the same carbon fibre content.

This comparison highlights the effectiveness of the material extrusion additive manufacturing method in producing CF/PPS composites with enhanced mechanical properties. The results from this study indicate that the 3D printed CF/PPS composites exhibit competitive performance when compared to traditionally manufactured CF/PPS composites. The use of carbon fibre fillers in the material process enhances the flexural strength of CF/PPS composites, making them a promising alternative for various applications requiring lightweight, high-strength and cost-effective materials. Overall, this study provides a comprehensive overview of the performance of the 3D printed CF/PPS composites and establishes their competitiveness in terms of flexural strength and modulus, which facilitates the development of high-performance CF/PPS composite parts with improved reliability and durability for demanding applications.

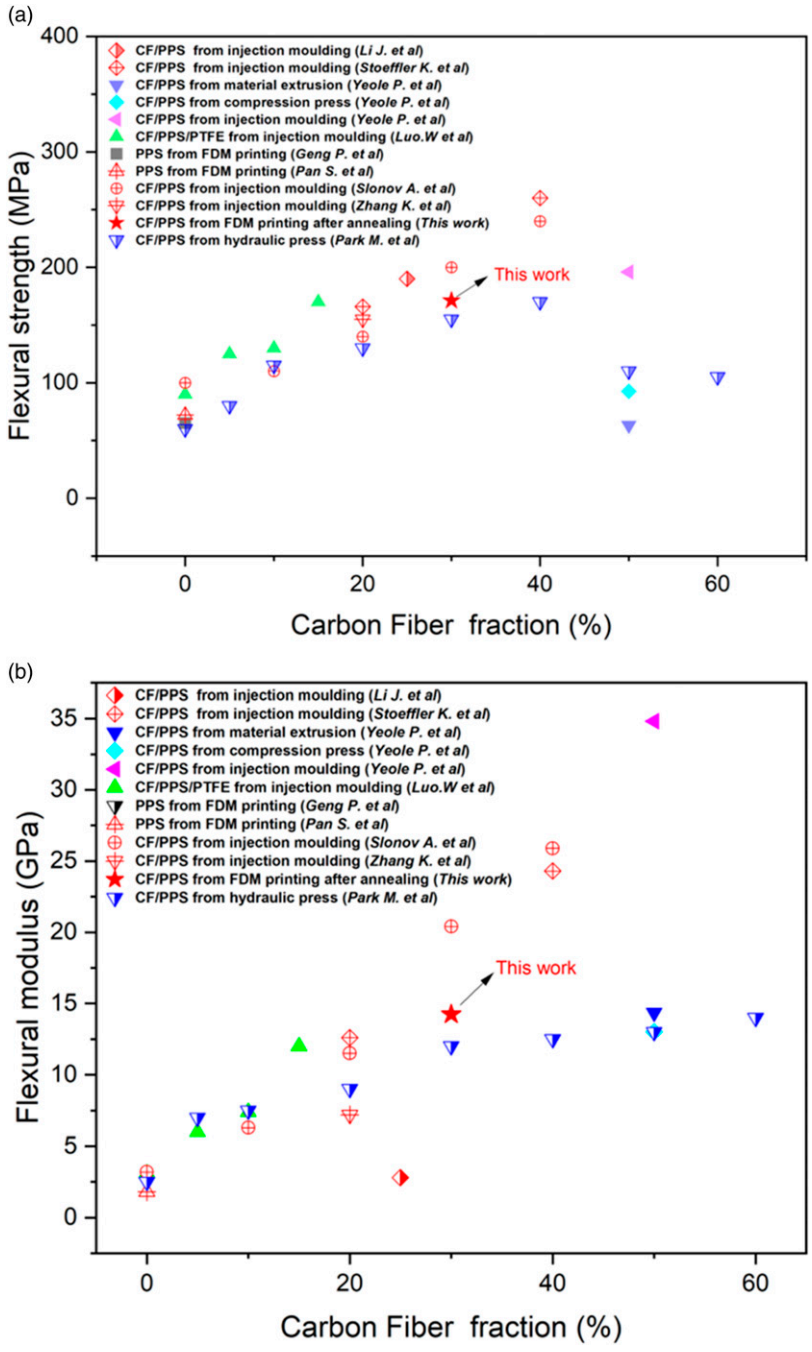

Figure 10. Comparison of (a) flexural strength and (b) flexural modulus in this work with previous studies.

Microstructural evolution of CF/PPS composites

The microstructure of the CF/PPS material, in terms of fibre weight fraction, fibre length, and air void contents, before and after 3D printing was measured. This was to check whether the microstructure has evolved in addition to the crystallinity of the PPS matrix, as they both could affect the mechanical properties of the printed CF/PPS composite. Optical microscopic images of the raw pellet, the filament, and the printed composite are shown in Figure 11(a), (c), and (e), respectively. Air void contents were measured using ImageJ software and listed in Table 1. It is shown that the void contents in both the raw pellets and the printed composites are around 5% although it becomes slightly higher (6.37%) in the extruded filaments. This is due to voids between the printed beads, even though the printer

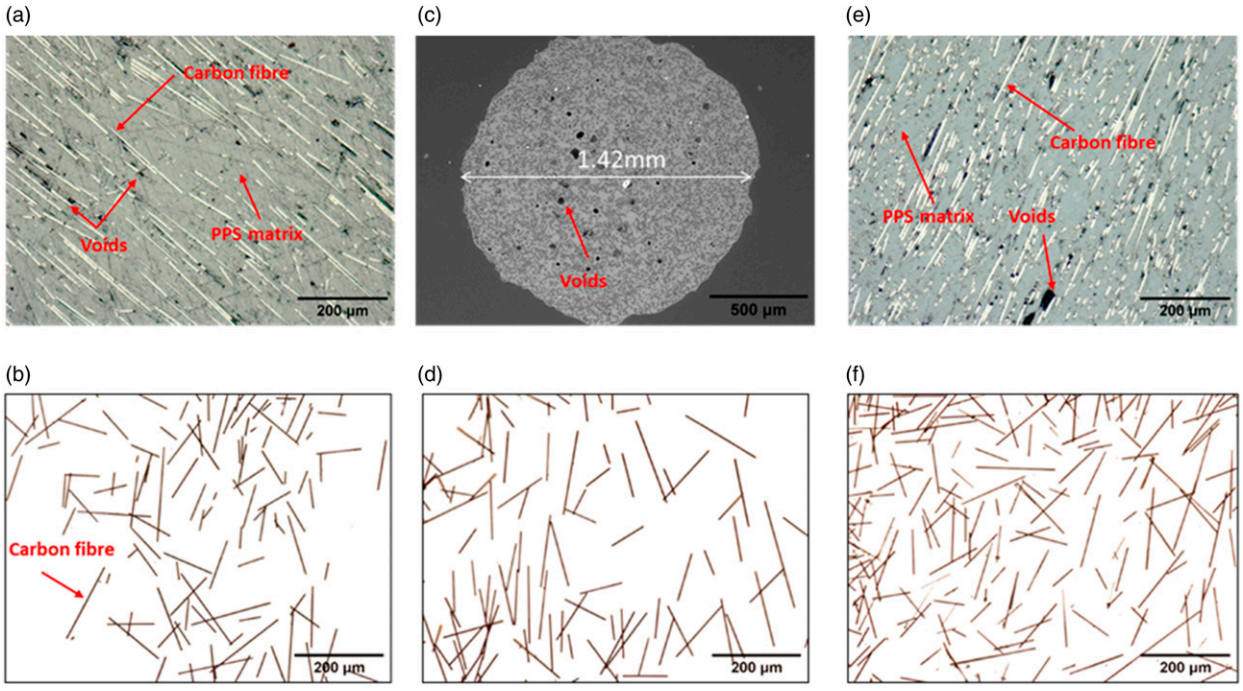

Figure 11. Cross-sectional images of (a) pellets (optical microscope: 10X), (c) filament (SEM: 150X) and (e) printed composites (optical microscope: 10X) and optical microscope images of carbon fibre in (b) pellets (optical microscope: 5X), (d) filament (optical microscope: 5X) and (f) printed composites (optical microscope: 5X) after pyrolysis.

Table 1. Summary of the carbon fibre length and carbon fibre volume and void content in raw pellets, extruded filaments, and printed composites.

	Carbon fibre length (µm)	Carbon fibre volume (%)	Void content (%)
Raw pellets	206.9 ± 106.0	28.6 ± 1.5	4.00 ± 0.80
Extruded filaments	209.5 ± 130.4	26.1 ± 1.2	6.37 ± 0.60
Printed composites	198.2 ± 144.6	25.3 ± 1.4	5.71 ± 0.64

nozzle diameter (0.8 mm) was smaller than the extruder nozzle diameter (1.75 mm). Nevertheless, the orientation angle of the discontinuous carbon fibres remains the same (18° in average) after being deposited through the 3D printer nozzle, as shown in Figure 11(e).

Samples of raw pellet, extruded filament, and printed composite were burned off in a furnace to thermally decompose the PPS matrix to measure the fibre weight fraction and fibre length. The pyrolysis conditions were set up to 500°C for 2 h to achieve a full decomposition of the PPS polymer. The results are shown in Figure 11(b), (d), and (f). The average fibre length was calculated by ImageJ software, and the fibre weight fraction was calculated by weighing the sample before and after pyrolysis. Both results are listed in Table 1. As seen in Table 1, there is no noticeable change in fibre length during the filament fabrication and material extrusion. The average fibre length remains around 200 µm in the CF/PPS filament and the printed CF/PPS composite. The fibre volume fraction was then calculated and found to be slightly reduced from 28.6% in the raw pellet to 26.1% in the filament and further to 25.3% in the printed composite. Overall, in the final printed composites, there is no substantial alteration of length and volume fraction of the discontinuous carbon fibres through the extrusion and printing processes, thus the effect of these parameters on the comparison of the flexural strength in each group is negligible.

Conclusions

This study provides valuable insights into the thermal processing conditions and their effects on CF/PPS material sin material extrusion. By optimizing the extrusion and printing parameters, we achieved the maximized flexural strength in the printed parts.

The results highlight the significant role of oxidation crosslinking reactions in altering the crystallinity and mechanical strength of CF/PPS composited at elevated temperatures. The findings indicate that oxidation crosslinking acts as a nucleating agent, enhancing the degree of crystallisation in uncross-linked polymers. However, at higher temperatures, the dominant effects of the linkage-like deconstruction of the polymer chains hider crystallisation.

Furthermore, the annealing treatment was found to influence the crystallisation process, thereby impacting the mechanical properties of the printed parts. Remarkably, the annealing thermal treatment showed a larger improvement in the mechanical properties of the printed CF/PPS composites with initially poorer properties.

In summary, this research provides a deeper scientific understanding of the relationship between thermal conditions, crystallinity, and mechanical performance in CF/PPS composites. The insights can guide future research in optimizing processing parameters and further enhancing the performance of CF/PPS composites in applications requiring lightweight, high-strength, and cost-effective materials.

Acknowledgements

Yahui Lyu would like to acknowledgment Edinburgh Global Research Scholarship and the Principal's Career Development Scholarship for financial support.

Author contributions

Yahui Lyu: Methodology, Writing – original draft, Formal analysis, Data curation. **Jiang Wu**: Resources, Software, Visualisation. **Haoqi Zhang**: Methodology, Visualization, Writing – Reviewing and Editing. **Conchúr M. Ó Brádaigh**: Writing – Reviewing and Editing, Supervision. **Dongmin Yang**: Conceptualization, Writing – Reviewing and Editing, Supervision.

Declaration of conflicting interests

The author(s) declared no potential conflicts of interest with respect to the research, authorship, and/or publication of this article.

Funding

The author(s) disclosed receipt of the following financial support for the research, authorship, and/or publication of this article: This work was supported by the University of Edinburgh.

ORCID iDs

Yahui Lyu https://orcid.org/0000-0002-6989-9304
Dongmin Yang https://orcid.org/0000-0002-4811-5443

Data availability statement

Data will be available on request.

References

1. Blok LG, Longana ML, Yu H, et al. An investigation into 3D printing of fibre reinforced thermoplastic composites. *Addit Manuf* 2018; 22: 176–186.
2. Ingen V, Wijngaarden V and Iii S. Development of the gulfstream G650 induction welded thermoplastic elevators and rudder. In: Sampe Seattle 2010, Seattle, WA, 17–20 May 2010. https://www.researchgate.net/publication/332403057
3. Geng P, Zhao J, Gao Z, et al. Effects of printing parameters on the mechanical properties of high-performance polyphenylene sulfide three-dimensional printing. *3D Print Addit Manuf* 2021; 8: 33–41.
4. Zuo P, Tcharkhtchi A, Shirinbayan M, et al. Overall investigation of poly (phenylene sulfide) from synthesis and process to applications—a review. *Macromol Mater Eng* 2019; 304: 1800686.
5. Ngo TD, Kashani A, Imbalzano G, et al. Additive manufacturing (3D printing): a review of materials, methods, applications and challenges. *Compos B Eng* 2018; 143: 172–196.
6. Brenken B, Barocio E, Favaloro A, et al. Fused filament fabrication of fiber-reinforced polymers: a review. *Addit Manuf* 2018; 21: 1–16.
7. McLouth TD, Severino JV, Adams PM, et al. The impact of print orientation and raster pattern on fracture toughness in additively manufactured ABS. *Addit Manuf* 2017; 18: 103–109.
8. Ferreira RTL, Amatte IC, Dutra TA, et al. Experimental characterization and micrography of 3D printed PLA and PLA reinforced with short carbon fibers. *Compos B Eng* 2017; 124: 88–100.
9. Zhang H, Wu J, Robert C, et al. 3D printing and epoxy-infusion treatment of curved continuous carbon fibre reinforced dual-polymer composites. *Compos B Eng* 2022; 234: 109687. DOI: 10.1016/j.compositesb.2022.109687.
10. Bhandari S, Lopez-Anido RA and Gardner DJ. Enhancing the interlayer tensile strength of 3D printed short carbon fiber reinforced PETG and PLA composites via annealing. *Addit Manuf* 2019; 30: 100922. DOI: 10.1016/j.addma.2019.100922.
11. Love LJ, Kunc V, Rios O, et al. The importance of carbon fiber to polymer additive manufacturing. *J Mater Res* 2014; 29: 1893–1898.
12. Van de Werken N, Tekinalp H, Khanbolouki P, et al. Additively manufactured carbon fiber-reinforced composites: state of the art and perspective. *Addit Manuf* 2020; 31: 100962.
13. Luo W, Liu Q, Li Y, et al. Enhanced mechanical and tribological properties in polyphenylene sulfide/polytetrafluoroethylene composites reinforced by short carbon fiber. *Compos B Eng* 2016; 91: 579–588.
14. Blok LG, Longana ML and Woods BKS. Fabrication and characterisation of aligned discontinuous carbon fibre reinforced thermoplastics as feedstock material for fused filament fabrication. *Materials* 2020; 13: 4671.

15. Lona Batista N, Anagnostopoulos K, Cocchieri Botelho E, et al. Influence of crystallinity on interlaminar fracture toughness and impact properties of polyphenylene sulfide/carbon fiber laminates. *Eng Fail Anal* 2021; 119: 104976. DOI: 10.1016/j.engfailanal.2020.104976.
16. El Magri A, Vaudreuil S, El Mabrouk K, et al. Printing temperature effects on the structural and mechanical performances of 3D printed poly-(phenylene sulfide) material. *IOP Conf Ser Mater Sci Eng* 2020; 783(1): 012001. DOI: 10.1088/1757-899X/783/1/012001.
17. Brenken B, Barocio E, Favaloro A, et al. Development and validation of extrusion deposition additive manufacturing process simulations. *Addit Manuf* 2019; 25: 218–226.
18. Barocio E, Brenken B, Favaloro A, et al. Interlayer fusion bonding of semi-crystalline polymer composites in extrusion deposition additive manufacturing. *Compos Sci Technol* 2022; 230: 109334. DOI: 10.1016/j.compscitech.2022.109334.
19. Garmabi MM, Shahi P, Tjong J, et al. 3D printing of polyphenylene sulfide for functional lightweight automotive component manufacturing through enhancing interlayer bonding. *Addit Manuf* 2022; 56: 102780. DOI: 10.1016/j.addma.2022.102780.
20. Kishore V, Chen X, Hassen AA, et al. Post-process annealing of large-scale 3D printed polyphenylene sulfide composites. *Addit Manuf* 2020; 35: 101387.
21. Fitzharris ER, Watanabe N, Rosen DW, et al. Effects of material properties on warpage in fused deposition modeling parts. *Int J Adv Manuf Technol* 2018; 95: 2059–2070.
22. Barocio E, Brenken B, Favaloro A, et al. Extrusion deposition additive manufacturing with fiber-reinforced thermoplastic polymers. *Structure and properties of additive manufactured polymer components*. Amsterdam, Netherlands: Elsevier Inc, 2020. DOI: 10.1016/b978-0-12-819535-2.00007-7.
23. Vaes D and Van Puyvelde P. Semi-crystalline feedstock for filament-based 3D printing of polymers. *Prog Polym Sci* 2021; 118: 101411.
24. El Magri A, El Mabrouk K, Vaudreuil S, et al. Optimization of printing parameters for improvement of mechanical and thermal performances of 3D printed poly(ether ether ketone) parts. *J Appl Polym Sci* 2020; 137: 49087. DOI: 10.1002/app.49625.
25. Geng P, Zhao J, Wu W, et al. Effect of thermal processing and heat treatment condition on 3D printing PPS properties. *Polymers* 2018; 10: 875. DOI: 10.3390/polym10080875.
26. Yang C, Tian X, Li D, et al. Influence of thermal processing conditions in 3D printing on the crystallinity and mechanical properties of PEEK material. *J Mater Process Technol* 2017; 248: 1–7.
27. Van de Voorde B, Katalagarianakis A, Huysman S, et al. Effect of extrusion and fused filament fabrication processing parameters of recycled poly(ethylene terephthalate) on the crystallinity and mechanical properties. *Addit Manuf* 2022; 50: 102518. DOI: 10.1016/j.addma.2021.102518.
28. Batista NL, Olivier P, Bernhart G, et al. Correlation between degree of crystallinity, morphology and mechanical properties of PPS/carbon fiber laminates. *Mat Res* 2016; 19: 195–201.
29. Deng S, Hou M and Ye L. Temperature-dependent elastic moduli of epoxies measured by DMA and their correlations to mechanical testing data. *Polym Test* 2007; 26: 803–813.
30. Paciornik S and d'Almeida J. Digital microscopy and image analysis applied to composite materials characterization. *Rev Mater* 2010; 15: 172–181.
31. Lee S, Kim D-H, Park J-H, et al. Effect of curing poly(*p*-phenylene Sulfide) on thermal properties and crystalline morphologies. *Adv Chem Eng Sci* 2013; 3: 145–149.
32. Wang L, Yu H, Chi Y, et al. Influence of thermal cross-linking temperature on the crystallization behavior of poly(phenylene sulfide). *Adv Polym Technol* 2015; 34(3): 21498. DOI: 10.1002/adv.21498.
33. Scobbo JJ and Hwang CR. Annealing effects in poly(phenylene sulfide) as observed by dynamic mechanical analysis. *Polym Eng Sci* 1994; 34(23): 1744–1749.
34. Liu Y, Zhou X and Wang Z. Effect of isothermal heat treatment on crystallinity, tensile strength and failure mode of CF/PPS laminate. *High Perform Polym* 2021; 33: 497–508.
35. Fan ZZ, He HW, Yan X, et al. Fabrication of ultrafine PPS fibers with high strength and tenacity via melt electrospinning. *Polymers* 2019; 11: 530. DOI: 10.3390/polym11030530.
36. Durani SMA, Khawaja EE, Masoudi HM, et al. IR laser ablative desulfurization of poly(1,4-phenylene sulfide). *J Anal Appl Pyrolysis* 2005; 73: 145–149.
37. Jian L and Tao S. The mechanical and tribological properties of CF/PPS composite filled with PA6. *J Thermoplast Compos Mater* 2014; 27: 594–602.
38. Stoeffler K, Andjelic S, Legros N, et al. Polyphenylene sulfide (PPS) composites reinforced with recycled carbon fiber. *Compos Sci Technol* 2013; 84: 65–71.
39. Yeole P, Hassen AA, Kim S, et al. Mechanical characterization of high-temperature carbon fiber-polyphenylene sulfide composites for large area extrusion deposition additive manufacturing. *Addit Manuf* 2020; 34: 101255. DOI: 10.1016/j.addma.2020.101255.
40. Pan S, Shen H and Zhang L. Effect of carbon nanotube on thermal, tribological and mechanical properties of 3D printing polyphenylene sulfide. *Addit Manuf* 2021; 47: 102247.
41. Zhang K, Zhang G, Liu B, et al. Effect of aminated polyphenylene sulfide on the mechanical properties of short carbon fiber reinforced polyphenylene sulfide composites. *Compos Sci Technol* 2014; 98: 57–63.
42. Park M, Park JH, Yang BJ, et al. Enhanced interfacial, electrical, and flexural properties of polyphenylene sulfide composites filled with carbon fibers modified by electrophoretic surface deposition of multi-walled carbon nanotubes. *Compos Part A Appl Sci Manuf* 2018; 109: 124–130.